

Dual Formulations of Mixed Finite Element Methods

ANDREW GILLETTE¹, CHANDRAJIT BAJAJ²

January 16, 2020

Abstract Mixed finite element methods solve a PDE using two or more variables. The theory of Discrete Exterior Calculus explains why the degrees of freedom associated to the different variables should be stored on both primal and dual domain meshes with a discrete Hodge star used to transfer information between the meshes. We show through analysis and examples that the choice of discrete Hodge star is essential to the numerical stability of the method. We also show how to define interpolation functions and discrete Hodge stars on dual meshes which can be used to create previously unconsidered mixed methods. Examples from magnetostatics and Darcy flow are examined in detail.

1 Introduction

The theory of Discrete Exterior Calculus (DEC) has provided a novel viewpoint for analyzing linear systems derived from finite element theory. We highlight three important conclusions of this theory:

1. Variables in a PDE should be discretized as degree of freedom arrays (“cochains”) over a primal simplicial mesh or its dual mesh.
2. A discrete Hodge star is used to transfer information between primal and dual meshes.
3. Whitney elements provide stable finite elements for the primal mesh.

Most numerical methods for PDEs over unstructured tetrahedral meshes discretize variables as cochains over the primal mesh and build up linear systems from there. In this paper, we look at the alternative approach of discretizing variables over the dual mesh and design dual formulations of the linear systems based on DEC theory. This approach is especially valuable in the context of mixed finite element systems as they employ all the key ingredients of DEC theory: both primal and dual cochains, a discrete Hodge star, and, typically, Whitney elements.

Before turning to mixed systems, however, we look at a simpler example from electromagnetics illustrating the relevance and benefit of our technique. The example is inspired by He and Teixeira [14]. Using a Discrete Exterior Calculus analysis of Maxwell’s equations, one can derive a second order vector wave equation

$$\mathbb{D}_1^T \mathbb{M}_2 \mathbb{D}_1 \mathbf{E} = \omega^2 \mathbb{M}_1 \mathbf{E}, \quad (1)$$

where \mathbf{E} is the electric field intensity, discretized as a cochain on the primal mesh, ω is a coefficient, \mathbb{D}_1 is a rectangular incidence matrix having entries of 0 and ± 1 only, and \mathbb{M}_k is a discrete Hodge star operator. The dual formulation of this physical phenomenon is an equation for the magnetic field intensity $\bar{\mathbf{H}}$, discretized as a cochain on the dual mesh:

$$\mathbb{D}_1 \mathbb{M}_1^{-1} \mathbb{D}_1^T \bar{\mathbf{H}} = \omega^2 \mathbb{M}_2^{-1} \bar{\mathbf{H}}. \quad (2)$$

Both systems (1) and (2) are computationally tractable if \mathbb{M}_k is a diagonal matrix which, by DEC theory, can be achieved when the primal and dual meshes are orthogonal. If orthogonality is not guaranteed, as is the case with barycentric dual meshes, \mathbb{M}_k is defined using Whitney elements and results in a sparse matrix. As a consequence, system (2) then involves possibly full rank matrices and is thus significantly more computationally expensive to solve. He and Teixeira [14] reduce the rank of the \mathbb{M}_k^{-1} matrices by using a topological thresholding technique which requires an input parameter.

Our approach skirts the problem of full rank inverses by introducing a novel definition of the \mathbb{M}_k^{-1} matrices free of parameters and guaranteed to produce a sparse matrix. The outline of the paper and summary of its contributions are as follows:

- In Section 2, we discuss prior work on Discrete Exterior Calculus, Whitney forms, generalized barycentric functions, and definitions of the discrete Hodge star. We introduce a combined DEC and deRham diagram to illustrate the interplay between primal and dual cochain spaces and the deRham sequence in \mathbb{R}^3 .
- In Section 3, we use the Sibson coordinate functions to construct dual Whitney-like functions which define a novel sparse inverse discrete Hodge star $(\mathbb{M}_k^{Dual})^{-1}$. We show how the choice of discrete Hodge star requires certain geometric quality conditions of the primal and dual mesh elements. We give a specific example showing how our dual formulation of the problem can result in a better conditioned linear system than the primal formulations.

¹ Department of Mathematics, University of Texas at Austin, agillette@math.utexas.edu

² Department of Computer Science, Institute for Computational Engineering and Sciences, University of Texas at Austin, bajaj@cs.utexas.edu

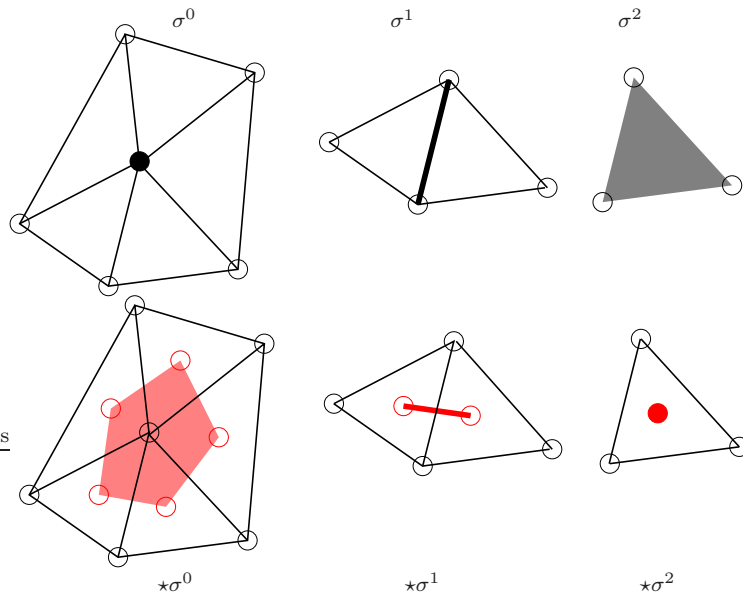


Fig. 1 Primal simplices are shown in black on the top row: σ^0 is a vertex, σ^1 is an edge, and σ^2 is a face. Their corresponding dual cells for $n = 2$ are shown in red on bottom: $\star\sigma^2$ is the barycenter of σ^2 , $\star\sigma^1$ is an edge between barycenters, and $\star\sigma^0$ is a planar polygon with barycenters as vertices. In three dimensions ($n = 3$), primal vertices have dual polytopes, primal edges have dual polygonal facets, primal faces have dual edges, and primal volumes have dual vertices.

- In Section 4, we examine how our methodology applies to generic PDE problems as well as to some specific applications employing mixed finite element methods. We cast each into our common notational framework and show how to formulate equivalent dual formulations of the problem from a DEC-based analysis. We discuss the specific advantages of these dual formulations, including an ability to confirm calculations on a primal mesh with the analogous calculations on the dual mesh.

2 Prior Work and Notation

2.1 Discrete Exterior Calculus

Discrete Exterior Calculus (DEC) is an attempt to create from scratch a discrete theory of differential geometry and topology whose definitions and theorems mimic their continuous counterparts [16, 2]. A central conclusion of the theory is that degrees of freedom for finite elements should be assigned to mesh vertices, edges, faces or interiors according to the dimensionality of the variable being modeled. If these degrees of freedom have a natural geometric duality, as occurs for example between electric and magnetic fields, two meshes of the domain are necessary - a primal and dual mesh [15]. This has given rise to DEC-based methods for solving problems of Darcy flow [17], electromagnetism [14] and elasticity [26], among others.

The primal domain mesh of an n -manifold is a simplicial complex K . We denote k -simplices by σ^k where $0 \leq k \leq n$. The dual domain mesh $\star K$ is defined by taking the circumcenters or barycenters of n -simplices and connecting them based on simplex adjacency in the usual manner. We denote dual k -cells by $\star\sigma^k$. Note that $\star\sigma^k$ is an $(n - k)$ -dimensional polytope and is associated to the k -dimensional simplex σ^k . The measure of σ^k (respectively $\star\sigma^{n-k}$) is denoted $|\sigma^k|$ (respectively $|\star\sigma^{n-k}|$), meaning length for $k = 1$, area for $k = 2$, and volume for $k = 3$, with the convention that $|\sigma^0| = |\star\sigma^n| = 1$. Examples for $n = 2$ are shown in Figure 1.

Pertinent definitions from DEC theory are summarized by the combined DEC and deRham diagram given in Figure 2 and described below. The vector space of k -cochains, i.e. linear mappings from k -simplices to \mathbb{R} , is denoted \mathcal{C}^k . The vector space of dual k -cochains, i.e. linear mappings from k -cells of the dual mesh to \mathbb{R} , is denoted $\bar{\mathcal{C}}^k$. These spaces are discrete analogues of Λ^k , the space of differential k -forms on the domain. The exterior derivative map $d_k : \Lambda^k \rightarrow \Lambda^{k+1}$ is used to define the deRham complex:

$$\Lambda^0 \xrightarrow{d_0} \Lambda^1 \xrightarrow{d_1} \dots \xrightarrow{d_{n-1}} \Lambda^n.$$

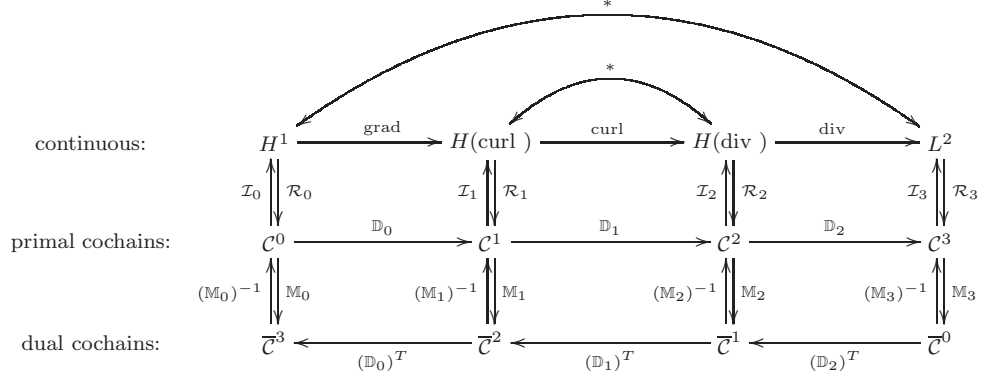


Fig. 2 The combined DEC and deRham diagram for a contractible domain in \mathbb{R}^3 .

In this work, we will focus on problems in \mathbb{R}^3 , in which the deRham complex becomes the more familiar sequence of finite element spaces and differential maps:

$$H^1 \xrightarrow{\text{grad}} H(\text{curl}) \xrightarrow{\text{curl}} H(\text{div}) \xrightarrow{\text{div}} L^2.$$

2.2 Whitney Forms

The interpolation map $\mathcal{I}_k : \mathcal{C}^k \rightarrow \Lambda^k$ converts k -cochains into k -forms with continuity prescribed by the deRham complex. We will use Whitney forms for these maps which were first described in [24] and later recognized by Bossavit [6] and others as the correct generalization of edge and face elements needed for DEC theory.

Whitney k -forms are piecewise linear functions on a primal mesh, one for each k -simplex in the mesh. The Whitney 0-form associated to a vertex $\sigma^0 := \mathbf{v}_i$ is denoted

$$\eta_{\sigma^0} := \lambda_i,$$

where λ_i is the barycentric function for the vertex. More precisely, λ_i is defined by the condition of being linear on every simplex of the mesh, subject to the constraints $\lambda_i(\mathbf{v}_j) = \delta_{ij}$. The Whitney 1-form associated to an oriented edge $\sigma^1 := [\mathbf{v}_i, \mathbf{v}_j]$ is the vector-valued function

$$\eta_{\sigma^1} := \lambda_i \nabla \lambda_j - \lambda_j \nabla \lambda_i. \quad (3)$$

The Whitney 2-form associated to an oriented face $\sigma^2 := [\mathbf{v}_i, \mathbf{v}_j, \mathbf{v}_k]$ is the vector-valued function

$$\eta_{\sigma^2} := 2 (\lambda_i \nabla \lambda_j \times \nabla \lambda_k + \lambda_j \nabla \lambda_k \times \nabla \lambda_i + \lambda_k \nabla \lambda_i \times \nabla \lambda_j)$$

The Whitney 3-form associated to an oriented tetrahedron σ^3 is its characteristic function, i.e.

$$\eta_{\sigma^3} := \chi_{\sigma^3} = \begin{cases} 1 & \text{on } \sigma^3 \\ 0 & \text{otherwise} \end{cases}$$

The Whitney interpolant \mathcal{I}_k of a k -cochain ω , is

$$\mathcal{I}_k(\omega) := \sum_{\sigma^k \in \mathcal{C}_k} \omega(\sigma^k) \eta_{\sigma^k}. \quad (4)$$

2.3 Generalized Barycentric Functions

It is evident from Figure 2 that the Whitney forms only map primal cochains to piecewise smooth functions. Since we are interested in defining Whitney-like interpolation functions for dual cochains, we first survey prior work on generalizing the lowest order Whitney forms, i.e. barycentric functions. We define the generalization precisely.

Definition 1 Let \mathcal{T} be a top-dimensional cell of the dual mesh (i.e. a polygon in 2D or a polyhedron in 3D) with vertices $\mathbf{v}_1, \dots, \mathbf{v}_N$. A set of functions $\bar{\lambda}_i : \mathcal{T} \rightarrow \mathbb{R}$, $i = 1, \dots, N$ are called **barycentric coordinates** on \mathcal{T} if they satisfy two properties.

- B1. **Non-negative:** $\bar{\lambda}_i \geq 0$.
 B2. **Linear Completeness:** For any linear function $L : \mathcal{T} \rightarrow \mathbb{R}$,

$$L = \sum_{i=1}^N L(\mathbf{v}_i) \bar{\lambda}_i.$$

A set of barycentric coordinates $\{\bar{\lambda}_i\}$ also satisfies these additional familiar properties:

- B3. **Partition of unity:** $\sum_{i=1}^N \bar{\lambda}_i \equiv 1$.
 B4. **Linear precision:** $\sum_{i=1}^N \mathbf{v}_i \bar{\lambda}_i(\mathbf{x}) = \mathbf{x}$.
 B5. **Interpolation:** $\bar{\lambda}_i(\mathbf{v}_j) = \delta_{ij}$.

A proof that properties B3-B5 are implied by B1-B2 in the 2D case can be found in our paper [13].

Three major approaches to defining generalized barycentric functions on 2D polygons have emerged in the literature. The Wachspress functions [21, 12] are rational functions constructed explicitly based on the areas of certain triangles within \mathcal{T} . The Sibson functions [19], also called the natural neighbor or natural element coordinates [20], are also constructed explicitly, but instead use the areas of Voronoi regions associated with the vertices of \mathcal{T} . The Harmonic functions [23, 8] are defined as the solution to Laplace's equation over \mathcal{T} with certain piecewise linear boundary data.

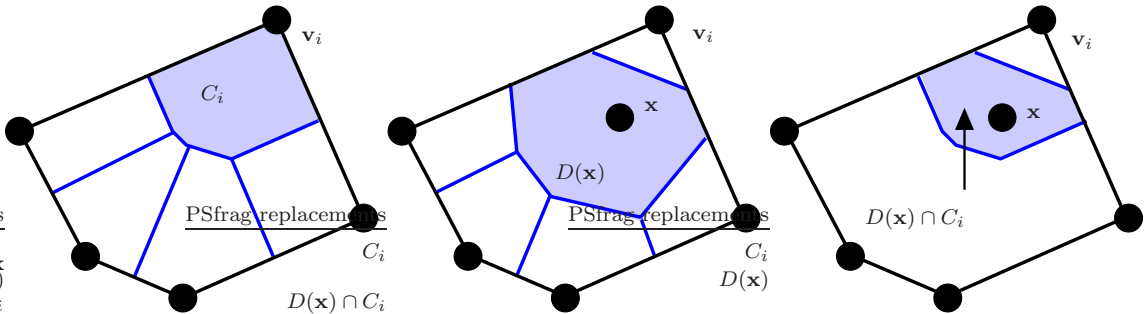


Fig. 3 Geometric calculation of a Sibson coordinate. C_i is the area of the Voronoi region associated to vertex \mathbf{v}_i inside \mathcal{T} . $D(\mathbf{x})$ is the area of the Voronoi region associated to \mathbf{x} if it is added to the vertex list. The quantity $D(\mathbf{x}) \cap C_i$ is exactly $D(\mathbf{x})$ if $\mathbf{x} = \mathbf{v}_i$ and decays to zero as \mathbf{x} moves away from \mathbf{v}_i , with value identically zero at all vertices besides \mathbf{v}_i .

We have shown in [13] that any of these functions suffice to give the optimal interpolation estimate for the lowest order case in 2D, assuming some basic geometric quality criteria on the dual mesh elements. For this paper, we will employ only the Sibson coordinates as they generalize easily to 3D, are reasonable to implement, and are more stable against bad geometry than the Wachspress functions. A formal proof of their convergence properties in 3D will be the focus of a future work.

To define the Sibson functions, let \mathbf{x} be a point inside a polyhedral cell \mathcal{T} of the dual mesh. Let P denote the set of vertices $\{\mathbf{v}_i\}$ and define

$$P' = P \cup \{\mathbf{x}\} = \{\mathbf{v}_1, \dots, \mathbf{v}_N, \mathbf{x}\}.$$

We denote the **Voronoi cell** associated to a point \mathbf{p} in a pointset Q by

$$V_Q(\mathbf{p}) := \{\mathbf{y} \in \mathcal{T} : |\mathbf{y} - \mathbf{p}| < |\mathbf{y} - \mathbf{q}|, \forall \mathbf{q} \in Q \setminus \{\mathbf{p}\}\}.$$

Note that these Voronoi cells have been restricted to \mathcal{T} and are thus always of finite size. We fix the notation

$$\begin{aligned} C_i &:= |V_P(\mathbf{v}_i)| = |\{\mathbf{y} \in \mathcal{T} : |\mathbf{y} - \mathbf{v}_i| < |\mathbf{y} - \mathbf{v}_j|, \forall j \neq i\}| \\ &= \text{area of cell for } \mathbf{v}_i \text{ in Voronoi diagram on the points of } P, \end{aligned}$$

$$\begin{aligned} D(\mathbf{x}) &:= |V_{P'}(\mathbf{x})| = |\{\mathbf{y} \in \mathcal{T} : |\mathbf{y} - \mathbf{x}| < |\mathbf{y} - \mathbf{v}_i|, \forall i\}| \\ &= \text{area of cell for } \mathbf{x} \text{ in Voronoi diagram on the points of } P'. \end{aligned}$$

By a slight abuse of notation, we also define

$$D(\mathbf{x}) \cap C_i := |V_{P'}(\mathbf{x}) \cap V_P(\mathbf{v}_i)|.$$

The notation is shown in Figure 3. The Sibson coordinates are defined to be

$$\bar{\lambda}_i(\mathbf{x}) := \frac{D(\mathbf{x}) \cap C_i}{D(\mathbf{x})} \quad \text{or, equivalently,} \quad \bar{\lambda}_i(\mathbf{x}) = \frac{D(\mathbf{x}) \cap C_i}{\sum_{j=1}^N D_j(\mathbf{x}) \cap C_j}.$$

Milbradt and Pick [18] modify the definition of the Sibson functions for polytopes so that an additional condition holds:

B6. Boundary agreement: If x lies on an edge (facet) and \mathbf{v}_i is not a vertex of the edge (facet) then $\bar{\lambda}_i(x) = 0$.

In other words, the coordinates of a point on an edge or facet of the polytope are dependent only on the Sibson functions associated to the boundary vertices of that edge or facet. This ensures C^0 continuity of the functions across adjacent mesh elements.

2.4 Discrete Hodge Star

As shown in Figure 2, the continuous Hodge star $*$ maps between forms of complementary and orthogonal dimensions, i.e. $*$: $\Lambda^k \rightarrow \Lambda^{n-k}$. For domains in \mathbb{R}^3 as considered here, $*$ is defined by the equations

$$*1 = dx dy dz, \quad *dx = dy dz, \quad *dy = -dx dz, \quad *dz = dx dy, \quad ** = 1.$$

For a more general definition of $*$, see [1].

A discrete Hodge star \mathbb{M} maps not only between cochains of complementary dimensions but also between primal and dual meshes [15]. In this paper, we focus on the two definitions of a discrete Hodge star most relevant to DEC theory. The first is the diagonal discrete Hodge star defined by

$$(\mathbb{M}_k^{Diag})_{ij} := \frac{|\star \sigma_i^k|}{|\sigma_i^k|} \delta_{ij}. \quad (5)$$

The definition of \mathbb{M}_k^{Diag} fits nicely into DEC theory when the dual mesh is defined by taking circumcenters of the primal simplices, thus producing orthogonal meshes [9]. In practice, however, it is often desirable to use barycenters to define the dual mesh as this guarantees that σ^k will intersect $\star \sigma^k$ in the ambient space. A correction factor for this change is given by Auchmann and Kurz [3].

The more widely used approach for barycentric dual meshes employs Whitney interpolants in the definition of the discrete Hodge star:

$$(\mathbb{M}_k^{Whit})_{ij} := \left(\eta_{\sigma_i^k}, \eta_{\sigma_j^k} \right) = \int_K \eta_{\sigma_i^k} \cdot \eta_{\sigma_j^k} \quad (6)$$

The inner product here is the standard integration of scalar or vector valued functions over the domain. Dodziuk [11] originally proposed the definition of \mathbb{M}_k^{Whit} but it has been called the Galerkin Hodge [7] for its relation to finite element methods. Bell [4] has implemented linear solvers in a DEC context using \mathbb{M}_k^{Whit} for various k .

We note that many other discrete Hodge stars appear in the literature, including the combinatorial discrete Hodge star of Wardetzsky and Wilson [22, 25] and the metrized chain Hodge star of DiCarlo et al. [10]. To our knowledge, no authors have defined a discrete Hodge star using dual interpolatory functions as we propose in this work.

3 Dual Whitney Interpolants and Dual Discrete Hodge Stars

It is evident from the DEC-deRham diagram in Figure 2 that the direct interpolation of degrees of freedom on a dual mesh is not available in the common theory. Further, we have seen from the discussion in Section 2.4 that the definition of $(\mathbb{M}_k)^{-1}$ has only been implied from definitions of \mathbb{M}_k . We now define a set of interpolation functions $\bar{\mathcal{I}}$ analogous to the Whitney interpolants defined in (4) and use them to provide an explicit definition of a dual discrete Hodge star.

The 0-form associated to a dual vertex $\star\sigma^3 := \mathbf{v}_i$ is

$$\eta_{\star\sigma^3} := \bar{\lambda}_i,$$

the Sibson function for the vertex. The 1-form associated to an oriented dual edge $\star\sigma^2 := [\mathbf{v}_i, \mathbf{v}_j]$ is the vector-valued function

$$\eta_{\star\sigma^2} := \bar{\lambda}_i \nabla \bar{\lambda}_j - \bar{\lambda}_j \nabla \bar{\lambda}_i$$

Assigning a vector-valued function to an oriented dual face is more subtle as the face is in general not a triangle. The dual face $\star\sigma^1$ will have m vertices where m is the number of tetrahedra σ^3 sharing the edge σ^1 . To associate a single 2-form to the face, we take the vertices in groups of consecutive triples and average them:

$$\begin{aligned} \eta_{\star\sigma^1} := & \frac{1}{m} \sum_{i=0}^{m-1} (\bar{\lambda}_i \nabla \bar{\lambda}_{i+1} \times \nabla \bar{\lambda}_{i+2}) + (\bar{\lambda}_{i+1} \nabla \bar{\lambda}_{i+2} \times \nabla \bar{\lambda}_i) \\ & + (\bar{\lambda}_{i+2} \nabla \bar{\lambda}_i \times \nabla \bar{\lambda}_{i+1}), \end{aligned}$$

where indices are taken mod m . The 3-form $\eta_{\star\sigma^0}$ associated to a dual cell $\star\sigma^0$ is its characteristic function:

$$\eta_{\star\sigma^0} := \chi_{\star\sigma^0} = \begin{cases} 1 & \text{on } \star\sigma^0 \\ 0 & \text{otherwise} \end{cases}$$

We define the dual Whitney interpolant of a dual $(n-k)$ -cochain $\bar{\omega} \in \bar{\mathcal{C}}^{n-k}$ to be

$$\bar{\mathcal{I}}_{n-k}(\bar{\omega}) := \sum_{\star\sigma^k \in \bar{\mathcal{C}}_{n-k}} \bar{\omega}(\star\sigma^k) \eta_{\star\sigma^k}. \quad (7)$$

We use the dual interpolants to define a dual discrete Hodge star by

$$((\mathbb{M}_k^{Dual})^{-1})_{ij} := \left(\eta_{\star\sigma_i^k}, \eta_{\star\sigma_j^k} \right). \quad (8)$$

The inner product here is the standard integration of scalar or vector valued functions over the dual domain $\star K$. For instance, in the case $k=3$, we have

$$((\mathbb{M}_3^{Dual})^{-1})_{ij} := \left(\eta_{\star\sigma_i^3}, \eta_{\star\sigma_j^3} \right) = \int_{\star K} \bar{\lambda}_i \bar{\lambda}_j.$$

The formulation for other k values will similarly involve integrals of the $\bar{\lambda}_i$ functions.

Lemma 1 $(\mathbb{M}_k^{Dual})^{-1}$ is sparse.

Proof Observe that $\eta_{\star\sigma^k}$ has localized support by construction. Entry ij of $(\mathbb{M}_k^{Dual})^{-1}$ will be non-zero only if $\star\sigma_i^k$ and $\star\sigma_j^k$ are adjacent. Thus each row of the matrix will have at most as many non-zero entries as $\star\sigma_i^k$ has adjacent $n-k$ cells, meaning the matrix is sparse.

Lemma 1 does not hold if \mathbb{M}_k^{Dual} is replaced by \mathbb{M}_k^{Whit} as these sparse matrices typically have dense inverses. We note that $(\mathbb{M}_k^{Diag})^{-1}$ is trivially sparse since it is diagonal, however, it can only be employed when the meshes are orthogonal.

3.1 Local Structure of Discrete Hodge Stars

The continuous Hodge star $*$ is a local operator meaning its effect on a differential form evaluated at a particular point on a manifold depends only on the geometry of a local neighborhood of the point. The discrete Hodge star is thus required to be a local operator as well meaning the evaluation of \mathbb{M}_k on a basis cochain ω_i^k (1 on σ_i^k and 0 otherwise) should involve values on only a few simplices adjacent to σ_i^k . In the language of matrix theory, this requirement says \mathbb{M}_k should be sparse.

We now prove a more specific characterization of the sparsity structure of \mathbb{M}_k^{Whit} and $(\mathbb{M}_k^{Dual})^{-1}$.

Lemma 2 *Entry ij in \mathbb{M}_k^{Whit} is non-zero only if there exists $\sigma^n \in K$ such that σ^n has at least one vertex from σ_i^k and one vertex from σ_j^k .*

Proof Computing entry ij in \mathbb{M}_k^{Whit} involves [5] summing terms of the form

$$\left(\int_K \lambda_1 \lambda_2 \right) \det \left(V_I^T W_J \right) \quad (9)$$

where λ_1, λ_2 are barycentric functions associated to $v_1 \in \sigma_i^k, v_2 \in \sigma_j^k$, respectively; I is a list of k vertices from σ_i^k not including v_1 ; J is a list of k vertices from σ_j^k not including v_2 ; and V_I, W_J are $n \times k$ matrices. The p th column of V_I is the vector $\nabla \lambda_p$ where λ_p is the barycentric function associated to the p th entry in I . The q th column of W_J is the vector $\nabla \lambda_q$ where λ_q is the barycentric function associated to the q th entry in J .

Observe that the support of the barycentric function associated to vertex v is contained within the n -simplices touching v . Thus, if there is no σ^n with at least one vertex from σ_i^k and one vertex from σ_j^k , the λ_1 and λ_2 appearing in (9) will always have disjoint support, making the entry zero.

Using the same kind of reasoning, we have a similar result for our dual discrete Hodge star.

Lemma 3 *Entry ij in $(\mathbb{M}_k^{Dual})^{-1}$ is non-zero only if there exists $\star\sigma^0 \in \star K$ such that $\star\sigma^0$ has at least one vertex from $\star\sigma_i^k$ and one vertex from $\star\sigma_j^k$.*

The number of k -simplices in an n -simplex is $\binom{n+1}{k}$ which gives the following corollary.

Corollary 1 *Let $A(\sigma^k)$ denote the number of n -simplices in K incident on at least one vertex from σ^k . Then the number of non-zero entries in row i of \mathbb{M}_k^{Whit} or row i of $(\mathbb{M}_k^{Dual})^{-1}$ is at most $\binom{n+1}{k} A(\sigma_i^k)$.*

The bound can be sharpened for particular choices of n and k or if additional assumptions are made about K . As stated, however, the corollary provides a simple means for evaluating the computational expense of a particular discretization scheme as we will discuss in Section 4.

3.2 Numerical Stability

To maintain the numerical stability of a DEC-based method, the discrete Hodge star matrix should have a bounded condition number. Put differently, the entries of the matrix should be roughly the same order of magnitude. This requirement is frequently considered from the context of numerical analysis but is often absent from the literature on discrete operators.

The common thread in the geometrically-defined discrete Hodge stars such as \mathbb{M}_k^{Diag} is a measurement of the size of dual cells i.e. $|\star\sigma^k|$. This suggests that geometric criteria on primal elements alone will not be sufficient to control the condition number of the discrete Hodge star matrix. In particular, since ratios of primal to dual cells are computed, we must satisfy the following criteria:

- N1. Primal simplices σ^k satisfy geometric quality measures.
- N2. Dual cells $\star\sigma^k$ satisfy geometric quality measures.
- N3. The value of $|\star\sigma^k|/|\sigma^k|$ is bounded above and below.
- N4. The primal and dual meshes do not have large gradation of elements, i.e. $\min_i |\sigma_i^k|$ and $\max_i |\sigma_i^k|$ are the same order of magnitude and $\min_i |\star\sigma_i^k|$ and $\max_i |\star\sigma_i^k|$ are the same order of magnitude.

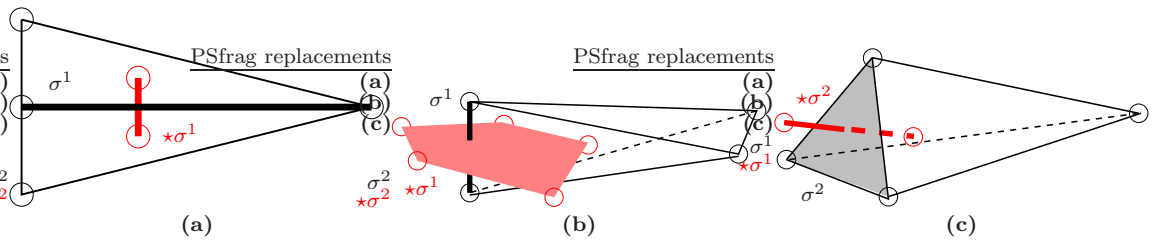


Fig. 4 Examples illustrating how the measure of a primal simplex σ^k (black) and its dual $\star\sigma^k$ (red) need not be the same order of magnitude. (a) In this 2D example, the ratio $|\star\sigma^1|/|\sigma^1|$ can be made arbitrarily small by increasing the length of σ^1 . (b) The ratio $|\star\sigma^1|/|\sigma^1|$ can be made arbitrarily large by decreasing the length of σ^1 . (c) The ratio $|\star\sigma^2|/|\sigma^2|$ can be made arbitrarily large by decreasing the area of σ^2 . Thus, a discrete Hodge star involving terms of the form $|\star\sigma^k|/|\sigma^k|$ may have a bad condition number unless primal *and* dual mesh quality is controlled.

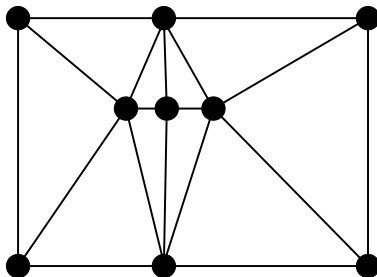


Fig. 5 Graded meshes also present a problem for discrete Hodge stars involving primal-dual size ratios. The primal mesh shown here induces a wide variation in values of $|\star\sigma^k|/|\sigma^k|$ for $k = 0, 1, 2$. This can cause ill-conditioned \mathbb{M}_k matrices, resulting in numerical instability.

Conditions N1 and N2 are required for discretization stability. Aspect ratio is often used as a geometric quality measure for tetrahedra. Conditions N3 and N4 are based on our analysis above. Condition N4 particular shows that these discrete Hodge stars are not fit for use on meshes tailored to multi-resolution situations where gradation is necessary to achieve reasonable computation times. We show some examples in Figures 4 and 5.

For \mathbb{M}_k^{Whit} , the size of the matrix entries are controlled by the size of the inner products of Whitney basis forms. The integrals in (9) are on the order of the size of $|\sigma_k|$, meaning again that a large gradation in primal mesh element size could produce large condition numbers and hence numerical instability. Since it does not involve the size of dual mesh elements, however, \mathbb{M}_k^{Whit} is more numerically stable against violations of conditions N2 and N3. Analogously, $(\mathbb{M}_k^{Dual})^{-1}$ is more numerically stable against violations of conditions N1 and N3. We summarize our conclusions below.

- \mathbb{M}_k^{Diag} may produce numerical instability if any of conditions N1-N4 are not satisfied.
- \mathbb{M}_k^{Whit} may produce numerical instability if conditions N1 or N4 are not satisfied.
- $(\mathbb{M}_k^{Dual})^{-1}$ may produce numerical instability if conditions N2 or N4 are not satisfied

3.3 Improved Condition Numbers with $(\mathbb{M}_k^{Dual})^{-1}$

To provide concrete evidence for our numerical stability claims, we present a simple example in 2D showing how \mathbb{M}_1^{Diag} and \mathbb{M}_1^{Whit} can have condition numbers an order of magnitude worse than $(\mathbb{M}_1^{Dual})^{-1}$ on the same mesh. This serves as a proof of concept that the DEC-based dual formulation of a problem can provide practical advantages in cases of difficult mesh geometry.

In the 2D mesh shown in Figure 6, the labeled vertices of the primal mesh have coordinates $\mathbf{v}_1 = (0, 0)$, $\mathbf{v}_2 = (0, 1)$, $\mathbf{v}_3 = (P, \frac{1}{2})$, and $\mathbf{v}_4 = (-P, \frac{1}{2})$, where P is a free parameter we can adjust to modify the geometry. The remaining vertices are chosen so that they form equilateral triangles with edges σ_{13} , σ_{23} , σ_{14} , and σ_{24} , as shown. The orthogonal, circumcenter-based dual mesh is shown in red.

Without loss of generality, fix any ordering on the mesh edges, beginning with

$$\{\sigma_{12}, \sigma_{13}, \sigma_{14}, \sigma_{23}, \sigma_{24}, \dots\}. \quad (10)$$

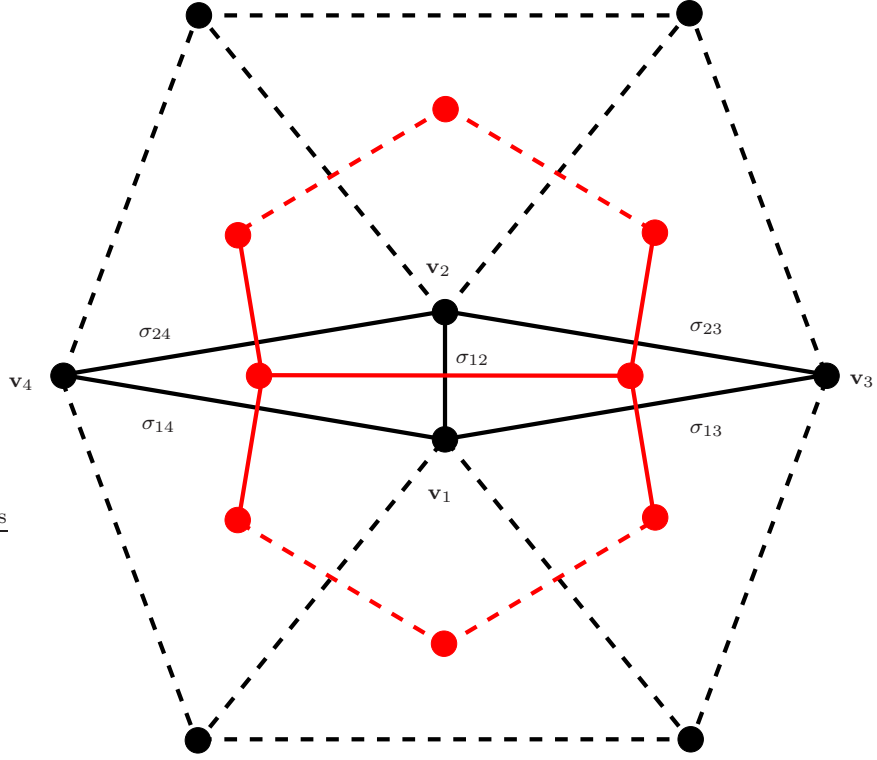


Fig. 6 Mesh used for sample calculation of \mathbb{M}_1 matrices. The vertices have coordinates $\mathbf{v}_1 = (0, 0)$, $\mathbf{v}_2 = (0, 1)$, $\mathbf{v}_3 = (P, \frac{1}{2})$, $\mathbf{v}_4 = (-P, \frac{1}{2})$.

We first calculate the upper left 5×5 block of each matrix, yielding the matrix values assigned to all possible interactions between pairs of these first five edges. Using the circumcentric dual mesh and definition (5), we compute

$$\mathbb{M}_1^{Diag} = \begin{pmatrix} \frac{4P^2 - 1}{4P} & 0 & 0 & 0 & 0 & \cdots \\ 0 & \varrho & 0 & 0 & 0 & \cdots \\ 0 & 0 & \varrho & 0 & 0 & \cdots \\ 0 & 0 & 0 & \varrho & 0 & \cdots \\ 0 & 0 & 0 & 0 & \varrho & \cdots \\ \vdots & \vdots & \vdots & \vdots & \vdots & \ddots \end{pmatrix} \quad (11)$$

where $\varrho = \frac{1}{4P^4} + \frac{P}{\sqrt{3+12P^2}}$. Since \mathbb{M}_1^{Diag} is diagonal, its condition number is the ratio of its largest diagonal entry to its smallest. The uncomputed diagonal entries will be very close to ϱ meaning the condition number can be approximated as

$$\text{cond}(\mathbb{M}_1^{Diag}) \approx \frac{4P^2 - 1}{4P} / \varrho \in O(P).$$

Using the Whitney interpolant for edges defined in (3) and the definition of \mathbb{M}_1^{Whit} given in (6), we can also compute

$$\mathbb{M}_1^{Whit} = \begin{pmatrix} \alpha & \beta & \beta & \beta & \beta & \cdots \\ \beta & \gamma & 0 & \delta & 0 & \cdots \\ \beta & 0 & \gamma & 0 & \delta & \cdots \\ \beta & \delta & 0 & \gamma & 0 & \cdots \\ \beta & 0 & \delta & 0 & \gamma & \cdots \\ \vdots & \vdots & \vdots & \vdots & \vdots & \ddots \end{pmatrix} \quad (12)$$

where $\alpha = \frac{12P^2+1}{24P}$, $\beta = \frac{4P^2-1}{48P}$, $\gamma = \frac{12P^2+20\sqrt{3}P+21}{144P}$, and $\delta = \frac{4P^2-5}{48P}$. We note that some of the structure of \mathbb{M}_1^{Whit} suggested by (12) is an artifice of our ordering of the edges as stated in (10). However, the remaining diagonal entries of \mathbb{M}_1^{Whit} are all close to γ , the entire matrix is symmetric, and the remaining non-zero off-diagonal terms are roughly the same size. Thus, the eigenvalues of the 5×5 matrix shown in (12) allow us to approximate the condition number of \mathbb{M}_1^{Whit} . Using Mathematica, we find analytical expressions for the max and min eigenvalues of the 5×5 matrix and take their ratio to approximate

$$\text{cond}(\mathbb{M}_1^{Whit}) \approx \frac{24P^2 + 5\sqrt{3}P + \sqrt{288P^4 - 120\sqrt{3}P^3 + 3P^2 + 9} + 3}{10\sqrt{3}P + 18} \in O(P)$$

Finally, we compute $(\mathbb{M}_1^{Dual})^{-1}$ using the barycentric dual mesh and definition (8), yielding

$$(\mathbb{M}_1^{Dual})^{-1} = \begin{pmatrix} \vartheta & \zeta & \zeta & \zeta & \zeta & \cdots \\ \zeta & \theta & \kappa & \xi & 0 & \cdots \\ \zeta & \kappa & \theta & 0 & \xi & \cdots \\ \zeta & \xi & 0 & \theta & \kappa & \cdots \\ \zeta & 0 & \xi & \kappa & \theta & \cdots \\ \vdots & \vdots & \vdots & \vdots & \vdots & \ddots \end{pmatrix} \quad (13)$$

where $\vartheta = (\eta_{\star\sigma_{12}^1}, \eta_{\star\sigma_{12}^1})$, $\zeta = (\eta_{\star\sigma_{12}^1}, \eta_{\star\sigma_{13}^1})$, $\theta = (\eta_{\star\sigma_{13}^1}, \eta_{\star\sigma_{13}^1})$, $\kappa = (\eta_{\star\sigma_{13}^1}, \eta_{\star\sigma_{14}^1})$ and $\xi = (\eta_{\star\sigma_{13}^1}, \eta_{\star\sigma_{23}^1})$. Note that analytical expressions of these inner products are not feasible due to the need to compute areas of intersection of irregular polygons in the definition of the $\bar{\lambda}$ functions. Instead, using Matlab, we create a simple grid-based quadrature method to estimate the entries of $(\mathbb{M}_1^{Dual})^{-1}$ for various values of P . As with \mathbb{M}_1^{Whit} , we then estimate the condition number of the entire matrix by the ratio of the max and min eigenvalues of the 5×5 matrix given in (13).

We tested the cases $P = 2, 5$, and 10 . The integral required to compute ξ has support outside of the portion of the dual mesh shown in Figure 6. We thus set ξ to be the same as ζ , since both are inner products associated to adjacent edges in the dual mesh. The computed values of κ were very small, as expected; we found that setting κ to zero did not affect the condition number estimate. Our results are summarized in Table 1.

P	$\text{cond}(\mathbb{M}_1^{Diag})$	$\text{cond}(\mathbb{M}_1^{Whit})$	$\text{cond}((\mathbb{M}_1^{Dual})^{-1})$
2	6.3	3.2	1.5
5	17.2	9.9	1.3
10	34.6	21.6	1.4

Table 1 Comparison of condition numbers of different discrete Hodge stars for various values of P .

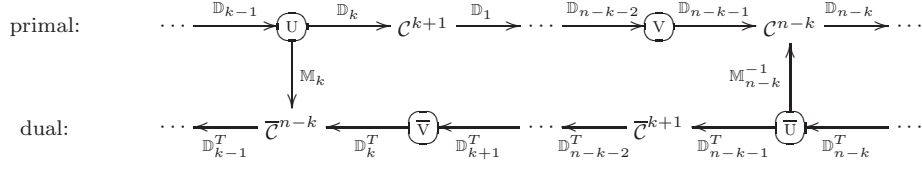


Fig. 7 Portion of a generic DEC-deRham diagram (cf. Figure 2) showing the natural duality between the variables and operators of systems (14) and (15). Discretizations of the variables are written in place of the primal or dual cochain spaces to which they belong.

Our numerical experiments thus provide evidence for the claim

$$\text{cond} \left((\mathbb{M}_1^{Dual})^{-1} \right) \in O(1).$$

The above example confirms that while our dual discrete Hodge star has an analogous definition to the primal discrete Hodge star, its condition number is indeed controlled by the geometric properties of the dual mesh elements, not those of the primal mesh elements. This fact is especially useful for problems on tetrahedral meshes where slivers (narrow, nearly planar tetrahedra) frequently occur and are difficult to remove.

4 Applications

The dual interpolation functions $\bar{\mathcal{I}}_{n-k}$ we defined in (7) and the dual discrete Hodge star we defined in (8) are new tools for designing stable finite element methods. We start by explaining the generic methodology of our approach and then apply it to two sample finite element problems from the literature: magnetostatics and Darcy flow.

4.1 Generic methodology

The Discrete Exterior Calculus approach to discretizing a PDE is as follows:

- I. **Translate** the continuous problem into the language of exterior calculus.
- II. **Linearize** the problem, possibly by introducing an intermediary variable (i.e. a mixed method).
- III. **Discretize** the variables into cochains and the operators d and $*$ into \mathbb{D} and \mathbb{M} matrices, according to DEC theory.

Our methodology focuses on step III and exposes how there are often many natural choices for discretization in line with DEC theory. We consider the case where we are given a PDE in terms of a variable u which should be interpreted in the continuous setting as a k -form. We also assume that a mixed method is possible in which the intermediary variable v should be interpreted as an $n-k-1$ form. In this case, the typical linear mixed linear system is

$$\begin{pmatrix} -\mathbb{M}_k & \mathbb{D}_k^T \\ \mathbb{D}_k & 0 \end{pmatrix} \begin{pmatrix} \mathbb{U} \\ \bar{\mathbb{V}} \end{pmatrix} = \begin{pmatrix} \bar{\mathbb{F}} \\ \mathbb{G} \end{pmatrix}. \quad (14)$$

where $\mathbb{U} \in \mathcal{C}^k$, $\bar{\mathbb{V}} \in \bar{\mathcal{C}}^{n-k-1}$ are the discretized variables and $\bar{\mathbb{F}} \in \bar{\mathcal{C}}^{n-k}$, $\mathbb{G} \in \mathcal{C}^{k+1}$ are the discretized load data.

The simple idea at the heart of our technique is to swap the *type* of discretization (primal or dual) of each variable and then infer the rest of the system from DEC theory. Note that the cochain order of each variable should not change, only the mesh on which it is discretized. Hence, the dual formulation of system (14) is

$$\begin{pmatrix} -\mathbb{M}_{n-k}^{-1} & \mathbb{D}_{n-k-1} \\ \mathbb{D}_{n-k-1}^T & 0 \end{pmatrix} \begin{pmatrix} \bar{\mathbb{U}} \\ \mathbb{V} \end{pmatrix} = \begin{pmatrix} \bar{\mathbb{F}} \\ \mathbb{G} \end{pmatrix}. \quad (15)$$

where now $\bar{\mathbb{U}} \in \bar{\mathcal{C}}^k$, $\mathbb{V} \in \mathcal{C}^{n-k-1}$ are the discretized variables and $\bar{\mathbb{F}} \in \bar{\mathcal{C}}^{n-k}$, $\mathbb{G} \in \bar{\mathcal{C}}^{k+1}$ are the discretized load data. We show in Figure 7 how these two discretizations fit into a generic DEC-deRham diagram in a natural and complementary fashion.

Additional equivalent systems can be derived by using proxy variables in clever ways, e.g. solving for some $\mathbb{z} \in \mathcal{C}^{k-1}$ such that \mathbb{x} is defined uniquely by $\mathbb{x} = \mathbb{D}_{k-1}\mathbb{z}$. These systems are easiest to understand via the specific examples we now examine.

4.2 Magnetostatics

The magnetostatics problem is characterized by Gauss's law for magnetism, Ampère's law, and a constitutive relationship, respectively,

$$\operatorname{div} b = 0, \quad *b = h, \quad \operatorname{curl} h = j. \quad (16)$$

Here, j is a given current density and b and h both represent the magnetic field. It is assumed that the domain Ω is contractible with boundary Γ written as a disjoint union $\Gamma^e \cup \Gamma^h$ such that $\hat{n} \cdot b = 0$ on Γ^e and $\hat{n} \times h = 0$ on Γ^h .

A DEC-based treatment of the problem reveals canonical and symmetrical ways to put this into a mixed formulation linear system, depending on whether b is discretized as a primal or dual cochain. If we discretize b as a primal 2-cochain $B \in \mathcal{C}^2$ and h as a dual 1-cochain $\bar{H} \in \bar{\mathcal{C}}^1$, equations (16) become

$$\mathbb{D}_2 B = 0, \quad \mathbb{M}_2 B = \bar{H}, \quad \mathbb{D}_1^T \bar{H} = \bar{J}.$$

This allows for two possible mixed systems. The first is

$$\begin{pmatrix} -\mathbb{M}_2 & \mathbb{D}_2^T \\ \mathbb{D}_2 & 0 \end{pmatrix} \begin{pmatrix} B \\ \bar{P} \end{pmatrix} = \begin{pmatrix} -\bar{H}_0 \\ 0 \end{pmatrix}. \quad (17)$$

In this system, $\bar{H}_0 \in \bar{\mathcal{C}}^1$ is any dual 1-cochain satisfying $\mathbb{D}_1^T \bar{H}_0 = \bar{J}$ and \bar{H} is defined by $\bar{H} := \bar{H}_0 + \mathbb{D}_2^T \bar{P}$. Thus $\mathbb{D}_1^T \bar{H} = \mathbb{D}_1^T (\bar{H}_0 + \mathbb{D}_2^T \bar{P}) = \bar{J}$ is assured.

The second mixed system is

$$\begin{pmatrix} -\mathbb{M}_2^{-1} & \mathbb{D}_1 \\ \mathbb{D}_1^T & 0 \end{pmatrix} \begin{pmatrix} \bar{H} \\ A \end{pmatrix} = \begin{pmatrix} 0 \\ \bar{J} \end{pmatrix}. \quad (18)$$

In this system, B is defined by $B := \mathbb{D}_1 A$, so that $\mathbb{D}_2 B = \mathbb{D}_2 \mathbb{D}_1 A = 0$. For a fixed \bar{J} , systems (17) and (18) result in the same solution pair (B, \bar{H}) and were shown by Bossavit [7] to converge to the solution pair (b, h) to (16) as the size of mesh elements goes to zero.

We now consider a novel dual discretization approach by treating b as a dual 2-cochain $\bar{B} \in \bar{\mathcal{C}}^2$ and h as a primal 1-cochain $H \in \mathcal{C}^1$. The continuous problem (16) is now discretized by

$$\mathbb{D}_0^T \bar{B} = 0, \quad \bar{B} = \mathbb{M}_1 H, \quad \mathbb{D}_1 H = J.$$

The first mixed system of this dual formulation is

$$\begin{pmatrix} -\mathbb{M}_1^{-1} & \mathbb{D}_0 \\ \mathbb{D}_0^T & 0 \end{pmatrix} \begin{pmatrix} \bar{B} \\ P \end{pmatrix} = \begin{pmatrix} -H_0 \\ 0 \end{pmatrix}. \quad (19)$$

In this system, $H_0 \in \mathcal{C}^1$ is any primal 1-cochain satisfying $\mathbb{D}_1 H_0 = J$ and H is defined by $H := \mathbb{M}_1^{-1} B$. Thus $\mathbb{D}_1 H = \mathbb{D}_1 (H_0 + \mathbb{D}_0 P) = J$ is assured. The last system is

$$\begin{pmatrix} -\mathbb{M}_1 & \mathbb{D}_1^T \\ \mathbb{D}_1 & 0 \end{pmatrix} \begin{pmatrix} H \\ A \end{pmatrix} = \begin{pmatrix} 0 \\ J \end{pmatrix}, \quad (20)$$

where \bar{B} is defined by $\bar{B} := \mathbb{D}_1^T A$ so that $\mathbb{D}_0^T \bar{B} = \mathbb{D}_0^T \mathbb{D}_1^T A = 0$. For a fixed \bar{J} , systems (17) and (18) will result in the same solution pair (\bar{B}, H) . In a future work, we will show that these systems also converge to the solution pair (b, h) to (16) as the size of mesh elements goes to zero. Taking that for granted, we state the advantages of having all four systems (17), (18), (19), and (20) available for implementation.

First, observe that systems (17) and (18) make use of the \mathbb{M}_2 matrix and its inverse while (19) and (20) use the \mathbb{M}_1 matrix. If the diagonal Hodge star is used, then \mathbb{M}_2 requires good ratios between the size of primal faces and their dual edges while \mathbb{M}_1 requires good ratios between the size of primal edges and their dual faces. Thus, on unstructured meshes, one system may break numerically on a mesh that is acceptable for another system.

Second, if the Whitney Hodge star is used, \mathbb{M}_k^{-1} may be a full rank matrix, making systems (18) and (19) less attractive numerically. By constructing the dual discrete Hodge stars as proposed in this paper, these systems become sparse again by Lemma 1 and thus are available as a practical alternative.

Third, having four systems available for the same problem allows for rigorous error-checking and cross-confirmation of results. This is particularly valuable when physical experimental confirmation of the results is impossible or expensive.

4.3 Darcy Flow

The Darcy flow problem in \mathbb{R}^3 is

$$\begin{cases} f + \frac{k}{\mu} \nabla p = 0 & \text{in } \Omega, \\ \operatorname{div} f = \phi & \text{in } \Omega, \\ f \cdot \hat{n} = \psi & \text{on } \partial\Omega, \end{cases} \quad (21)$$

where k and μ are physical constants, f is volumetric flux and p is pressure. It is assumed that there is no external body force, the boundary $\Gamma := \partial\Omega$ is piecewise smooth, and the compatibility condition $\int_{\Omega} \phi d\Omega = \int_{\partial\Omega} \psi d\Gamma$ is satisfied. Without loss of generality, we take $\mu = k$.

First we consider discretizing f as a primal 2-cochain $F \in \mathcal{C}^2$ and p as a dual 0-cochain $\bar{P} \in \bar{\mathcal{C}}^0$, yielding the discretized equations

$$\mathbb{M}_2 F + \mathbb{D}_2^T \bar{P} = 0, \quad \mathbb{D}_2 F = \Phi.$$

Hirani et al. [17] used this approach to derive the linear system

$$\begin{pmatrix} \mathbb{M}_2 & \mathbb{D}_2^T \\ \mathbb{D}_2 & 0 \end{pmatrix} \begin{pmatrix} F \\ \bar{P} \end{pmatrix} = \begin{pmatrix} 0 \\ \Phi \end{pmatrix}. \quad (22)$$

We present an alternative formulation using the same discretization, inspired by the magnetostatics systems (18) and (20). Let $F_0 \in \mathcal{C}^2$ be a primal 2-cochain satisfying $\mathbb{D}_2 F_0 = \Phi$. The system is

$$\begin{pmatrix} -\mathbb{M}_2^{-1} & \mathbb{D}_1 \\ \mathbb{D}_1^T & 0 \end{pmatrix} \begin{pmatrix} \bar{Q} \\ G \end{pmatrix} = \begin{pmatrix} -F_0 \\ 0 \end{pmatrix}. \quad (23)$$

Here, \bar{P} is a solution to $\mathbb{D}_2^T \bar{P} = -\bar{Q}$. The existence of \bar{P} is guaranteed by the exactness of the dual cochain sequence at $\bar{\mathcal{C}}^1$ and uniqueness of \bar{P} is determined by initial conditions or boundary data. The flux cochain F is defined to be $\mathbb{M}_2^{-1} \bar{Q}$ so that $\mathbb{D}_2 F = \mathbb{D}_2(\mathbb{M}_2^{-1} \bar{Q}) = \mathbb{D}_2(F_0 + \mathbb{D}_1 G) = \Phi$.

We now present the dual formulations derived by treating f as a dual 2-cochain $\bar{F} \in \bar{\mathcal{C}}^2$ and p as a primal 0-cochain $P \in \mathcal{C}^0$. The discretized equations are now

$$\mathbb{M}_1^{-1} \bar{F} + \mathbb{D}_0 P = 0, \quad \mathbb{D}_0^T \bar{F} = \bar{\Phi}.$$

The first system of this formulation is

$$\begin{pmatrix} \mathbb{M}_1^{-1} & \mathbb{D}_0 \\ \mathbb{D}_0^T & 0 \end{pmatrix} \begin{pmatrix} \bar{F} \\ P \end{pmatrix} = \begin{pmatrix} 0 \\ \bar{\Phi} \end{pmatrix}. \quad (24)$$

The second system is

$$\begin{pmatrix} \mathbb{M}_1 & \mathbb{D}_1^T \\ \mathbb{D}_1 & 0 \end{pmatrix} \begin{pmatrix} Q \\ \bar{G} \end{pmatrix} = \begin{pmatrix} \bar{F}_0 \\ 0 \end{pmatrix}. \quad (25)$$

where \bar{F}_0 is a solution to $\mathbb{D}_0^T \bar{F}_0 = \bar{\Phi}$ and \bar{F} is defined to be $\mathbb{M}_1 Q$, analogous to system (23). Thus, taking \mathbb{D}_0^T of both sides of the top equation of (25) yields $\mathbb{D}_0^T \bar{F} = \bar{\Phi}$. Further, the bottom equation of (25) yields $\mathbb{D}_1 Q = 0$ which, by the exactness property of the primal cochain sequence implies that there exists a solution P to $\mathbb{D}_0 P = -Q$.

We now have four mixed systems, (22)-(25), discretizing the Darcy flow equations (21), three of which had not been considered by Hirani et al. [17]. This plethora of equivalent systems offers the same advantages as those discussed at the end of the magnetostatics example from Section 4.2.

5 Conclusion

In this work we have augmented the theories of Discrete Exterior Calculus and mixed methods by introducing two novel tools: Whitney-like interpolation functions defined on dual domain meshes and a sparse inverse discrete Hodge star. We have shown the tools to have natural, straightforward definitions and clear geometric interpretations. We have used the them to derive previously unexamined numerical stability criteria relating to the condition number of the discrete Hodge star used in the method, based on the geometry of the dual mesh cells. Further, we have demonstrated in both general and specific contexts how these tools can be used to develop alternative discretizations of PDEs with sparse, well-conditioned matrices. The techniques we have described provide a valuable methodology for researchers to revisit their current finite element formulations and confirm or improve their results with new discretization methods.

Acknowledgments We are grateful to Alexander Rand for his help in implementing the Sibson coordinates. This research was supported in part by NIH contracts R01-EB00487, R01-GM074258, and a grant from the UT-Portugal CoLab project.

References

1. R. Abraham, J. E. Marsden, and T. Ratiu. *Manifolds, tensor analysis, and applications*, volume 75 of *Applied Mathematical Sciences*. Springer-Verlag, New York, second edition, 1988.
2. D. Arnold, R. Falk, and R. Winther. Finite element exterior calculus, homological techniques, and applications. *Acta Numerica*, pages 1–155, 2006.
3. B. Auchmann and S. Kurz. A geometrically defined discrete hodge operator on simplicial cells. *Magnetics, IEEE Transactions on*, 42(4):643–646, April 2006.
4. W. N. Bell. Algebraic multigrid for discrete differential forms (dissertation). Technical report, University of Illinois at Urbana-Champaign, 2008.
5. W. N. Bell. Personal communication, 2008.
6. A. Bossavit. Mixed finite elements and the complex of Whitney forms. In J. Whiteman, editor, *The mathematics of finite elements and applications VI*, pages 137–144. Academic Press, 1988.
7. A. Bossavit. Computational electromagnetism and geometry (5). *Journal of the Japan Society of Applied Electromagnetics*, 8:203–209, 2000.
8. S. H. Christiansen. A construction of spaces of compatible differential forms on cellular complexes. *Math. Models Methods Appl. Sci.*, 18(5):739–757, 2008.
9. M. Desbrun, A. N. Hirani, M. Leok, and J. E. Marsden. Discrete Exterior Calculus. *arXiv:math/0508341*, 2005.
10. A. DiCarlo, F. Milicchio, A. Paoluzzi, and V. Shapiro. Discrete physics using metrized chains. In *2009 SIAM/ACM Joint Conference on Geometric and Physical Modeling*, pages 135–145. ACM, 2009.
11. J. Dodziuk. Finite-difference approach to the Hodge theory of harmonic forms. *Amer. J. Math.*, 98(1):79–104, 1976.
12. M. Floater, K. Hormann, and G. Kós. A general construction of barycentric coordinates over convex polygons. *Advances in Computational Mathematics*, 24(1):311–331, 2006.
13. A. Gillette, A. Rand, and C. Bajaj. Error estimates for generalized barycentric interpolation. *Advances in Computational Mathematics*, Submitted, 2010.
14. B. He and F. Teixeira. Geometric finite element discretization of maxwell equations in primal and dual spaces. *Physics Letters A*, 349(1-4):1 – 14, 2006.
15. R. Hiptmair. Discrete hodge-operators: an algebraic perspective. *Progress In Electromagnetics Research*, 32:247–269, 2001.
16. A. N. Hirani. Discrete exterior calculus (dissertation). Technical report, California Institute of Technology, 2003.
17. A. N. Hirani, K. B. Nakshatrala, and J. H. Chaudhry. Numerical method for Darcy flow derived using Discrete Exterior Calculus. *arXiv:0810.3434*, 2008.
18. P. Milbradt and T. Pick. Polytope finite elements. *International Journal for Numerical Methods in Engineering*, 73(12):1811–1835, 2008.
19. R. Sibson. A vector identity for the Dirichlet tessellation. *Math. Proc. Cambridge Philos. Soc.*, 87(1):151–155, 1980.
20. N. Sukumar and E. A. Malsch. Recent advances in the construction of polygonal finite element interpolants. *Archives of Computational Methods in Engineering*, 13(1):129–163, 2006.
21. E. L. Wachspress. *A Rational Finite Element Basis*, volume 114 of *Mathematics in Science and Engineering*. Academic Press, 1975.
22. M. Wardetzky. Discrete differential operators on polyhedral surfaces - convergence and approximation (dissertation). Technical report, Freie Universitt Berlin, 2006.
23. J. Warren, S. Schaefer, A. N. Hirani, and M. Desbrun. Barycentric coordinates for convex sets. *Advances in Computational Mathematics*, 27(3):319–338, 2007.
24. H. Whitney. *Geometric Integration Theory*. Princeton University Press, 1957.
25. S. O. Wilson. Cochain algebra on manifolds and convergence under refinement. *Topology Appl.*, 154(9):1898–1920, 2007.
26. A. Yavari. On geometric discretization of elasticity. *Journal of Mathematical Physics*, 49(2):022901–1–36, 2008.